Trim Drag Prediction for Blended-Wing-Body UAV Configuration

Deng Haiqiang (邓海强)[1], *Yu Xiongqing* (余雄庆)[2*],
Yin Hailian (尹海莲)[1], *Deng Feng* (邓枫)[2]

1. UAV Research Institute, Nanjing University of Aeronautics and Astronautics, Nanjing 210016, P. R. China;
2. Key Laboratory of Fundamental Science for National Defense Advanced Design Technology of Flight Vehicle, Nanjing University of Aeronautics and Astronautics, Nanjing 210016, P. R. China

(Received 12 December 2013; revised 7 January 2015; accepted 12 January 2015)

Abstract: A rapid method of the trim drag prediction for the blended-wing-body unmanned aerial vehicle (UAV) configuration is proposed. The method consists of four steps. The first step is to parameterizedly model the blended-wing-body UAV configuration; the second is to analyze the aerodynamics of the geometric model; the third is to create aerodynamic surrogate model; and the final step is to predict the trim drag using the surrogate model. Hence, a tool for trim drag prediction is developed by integration of the four steps. The impacts of the allocation of control surfaces, position of gravity center and planform parameters on the trim drag are investigated by using the tool. Results show that using the control surface in outer wing for trim has an advantage of lower trim drag, and the position of gravity center has a primary impact on the trim drag. Moreover, the planform has secondary impacts on the trim drag.

Key words: aerodynamic configuration; blended-wing-body; trim drag; unmanned aerial vehicles (UAVs)

CLC number: V212.11 **Document code**: A **Article ID**: 1005-1120(2015)01-0133-04

0 Introduction

The features of higher aerodynamic efficiency and lower observability[1-5] guarantee the blended-wing-body (BWB) an attractive configuration for unmanned aerial vehicles (UAVs). However, the trim and static margin are critical for the BWB configurations[3] due to the absence of a horizontal tail.

This paper addresses the trim drag issues of a subsonic BWB UAV. The trim drag is the increment in drag from aerodynamic trimming[6]. For BWB configurations, the trim drag comprises: (1) the profile drag increment due to control surface deflections; (2) the induced drag increment due to the change of lift distribution caused by the control surface deflections. The impacts of allocations of control surfaces, gravity center position and planform parameters on the trim drag are investigated. The baseline configuration of the UAV is shown in Fig. 1. The reference area S_w is 20 m^2, the aspect ratio $AR = 4.9$. The leading edges of inner wing and winglet are parallel, the same to the trailing edges of inner wing and opposite outer wing. The trailing edges of outer wing and winglet are coincident. The rapid method and tool for the trim drag prediction is presented. Furthermore, the impacts of parameters are discussed.

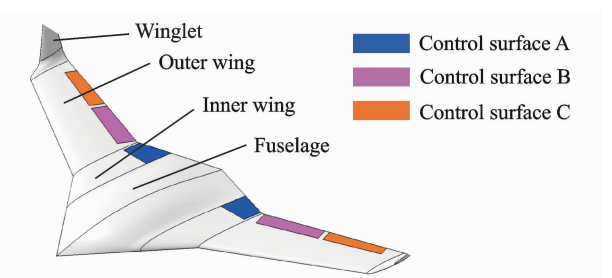

Fig. 1 Baseline configuration of BWB UAV

* **Corresponding author**: Yu Xiongqing, Professor, E-mail: yxq@nuaa.edu.cn.

How to cite this article: Deng Haiqiang, Yu Xiongqing, Yin Hailian, et al. Trim drag prediction for blended-wing-body UAV configuration[J]. Trans. Nanjing U. Aero. Astro., 2015, 32(1):133-136.
http://dx.doi.org/10.16356/j.1005-1120.2015.01.133

1 Computational Method

1.1 Geometry parameterization

A VB code is developed[7] to generate the geometry model by defining three sets of parameters.

(1) Planform parameters are listed as follows: the ratio of winglet's lateral projection area to reference area R_S, half of fuselage width $W_{Fuselage}$, the sweeping angles Λ_1, Λ_2 and Λ_3 of the the leading and trailing edge (Fig. 2), the dihedrals Γ_W and $\Gamma_{Winglet}$ of the wing and winglet.

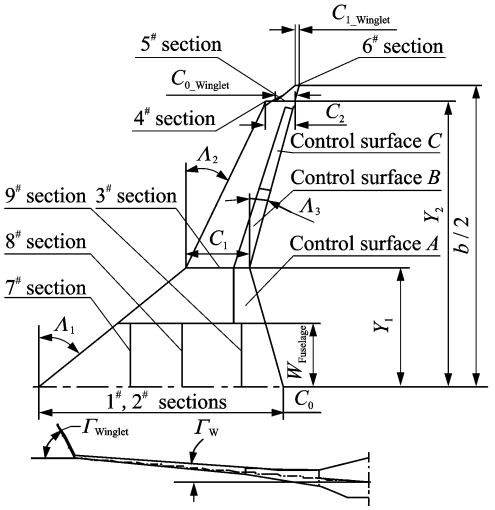

Fig. 2 Definition of configuration parameters

(2) Cross section parameters include the airfoils and twist angles of sections 1 to 6, as well as the parameters of sections 7 to 9. The method presented by Ref. [8] is used to parameterize these cross sections.

(3) Deflections of control surfaces are δ_A, δ_B, and δ_C for control surfaces A, B and C, respectively.

The absolute position of gravity center is normalized by the mean aerodynamic chord length C_{ac}

$$\bar{x}_{cg} = (x_{cg} - x_{(1/4)ac})/C_{ac} \tag{1}$$

where x_{cg} and $x_{(1/4)ac}$ are the x coordinate of gravity center and the quarter point of mean aerodynamic chord, respectively.

1.2 Grid generation and aerodynamic analysis

Two Gridgen scripts are programmed to generate the meshes for the geometries without and with the control surface deflections, respectively. After that, the panel method program PanAir[9] is ultilized to predict lift coefficient C_L, induced drag coefficient C_{Di} and pitching moment coefficient C_m.

1.3 Surrogate model for aerodynamic analysis

For each planform of the BWB UAV, the aerodynamic coefficients $C_L(\alpha, \delta_A, \delta_B, \delta_C)$, $C_{Di}(\alpha, \delta_A, \delta_B, \delta_C)$ and $C_m(\alpha, \delta_A, \delta_B, \delta_C)$ are computed by the above aerodynamic method. The radial basis function method[10] is utilized to create the aerodynamic surrogate model. It takes α, δ_A, δ_B, δ_C as input parameters and C_L, C_{Di}, C_m as output parameters.

1.4 Trim drag computation

The trim drag coefficient C_{D_trim} is given by

$$C_{D\_trim} = \Delta C_{D\_tr\_p} + \Delta C_{D\_tr\_w} \tag{2}$$

$$\Delta C_{D\_tr\_w} = C_{Di\_deflected} - C_{Di\_clean} \tag{3}$$

where $\Delta C_{D\_tr\_p}$ is the profile drag increment estimated by an engineering method[6], $\Delta C_{D\_tr\_w}$ the induced drag increment, C_{Di_clean} the induced drag coefficient of the clean configuration, and $C_{Di\_deflected}$ the induced drag coefficient in trimming condition obtained from an trimming optimization. The formulation of the optimization is to minimize the value of C_{D_trim} via design variables α, δ_A, δ_B, δ_C with the constraints of a fixed C_L, as well as $C_m = 0$.

1.5 Tool for trim drag computation

A tool for trim drag computation is developed by integrating the above steps within iSIGHT-FD software, and the workflow is shown in Fig. 3. The impact of each parameter listed in Table 1 on trim drag is investigated under the condition that others remain their baseline values by the proposed tool.

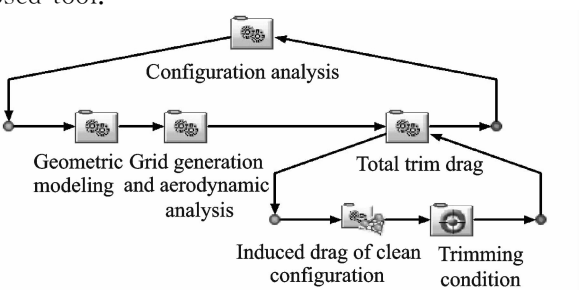

Fig. 3 Workflow for trim drag computation

Table 1 Baseline values and ranges of parameters

Parameter	Lower bound	Baseline	Upper bound
Λ_1/(°)	40	50	60
Λ_2/(°)	20	30.5	40
AR	4	4.9	7
$\bar{x}_{cg}$	−0.3	0.2	0.3

2 Results

2.1 Impact of control surface allocation

The trim drags for different allocations of control surfaces are listed in Table 2. The options A, B, C signify that only the control surface A, or B, or C is used for trim, respectively. "Hybrid" indicates that all the control surfaces are used simultaneously for trim. The results show that the option C has the lowest trim drag than the options A and B, thus simplifying the control system without remarkable trim drag penalty compared with the option "Hybrid".

Table 2 Trim drags for different allocations

Option	$\Delta C_{D\_tr\_p}$	$\Delta C_{D\_tr\_w}$	C_{D_trim}
A	3.58E−05	7.41E−07	3.66E−05
B	1.98E−05	−7.47E−06	1.24E−05
C	1.22E−05	−7.48E−06	4.70E−06
Hybrid	4.05E−04	−4.76E−04	−7.13E−05

2.2 Impact of gravity center position

The impact of $\bar{x}_{cg}$ on C_{D_trim} is plotted in Fig. 4. The value of $\Delta C_{D\_tr\_p}$ decreases with the increase of $\bar{x}_{cg}$ until $\bar{x}_{cg}$ is greater than 0.2. Subsequently it increases gradually. The reason is that the value of C_m changes from negative to positive when the parameter $\bar{x}_{cg}$ increases. Consequently, the δ_C increases from negative to positive and is almost zero when $\bar{x}_{cg}$ is equal to 0.2.

The $\Delta C_{D\_tr\_w}$ descends with the increase of $\bar{x}_{cg}$ when $\bar{x}_{cg}$ is less than 0.25, thereafter it increases slightly. It is because the nose-down moment and δ_C decrease with the increasing $\bar{x}_{cg}$ when $\bar{x}_{cg}$ is less than 0.2, and the spanwise lift distribution is more "ellipical". However, the spanwise lift distribution begins to depart from the elliptical shape when $\bar{x}_{cg}$ is greater than 0.25.

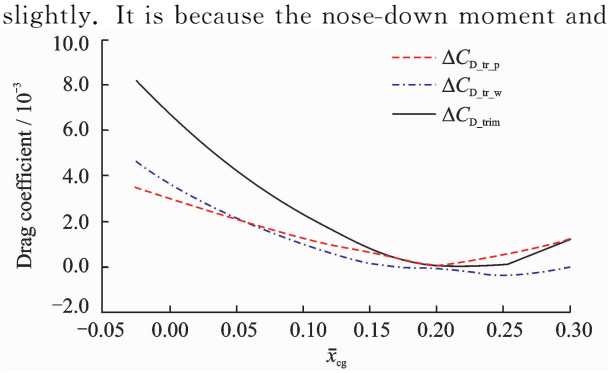

Fig. 4 Impact of gravity center position on trim drag

The C_{D_trim} drops rapidly when the $\bar{x}_{cg}$ is less than 0.2. After C_{D_trim} reaches its minimum at $\bar{x}_{cg}=0.2$, C_{D_trim} increases gradually along the positive direction of $\bar{x}_{cg}$ with values more than 0.2.

2.3 Impacts of planform parameters

2.3.1 Impact of inner wing leading edge sweep

The impact of Λ_1 on C_{D_trim} is depicted in Fig. 5.

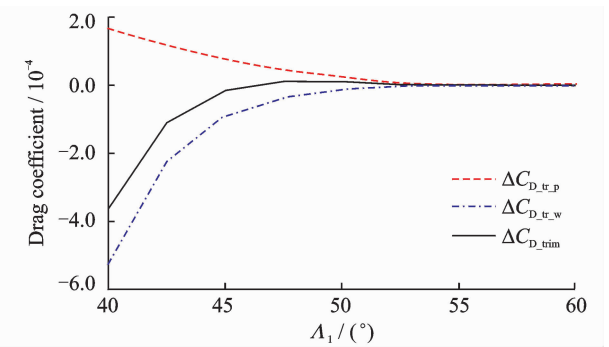

Fig. 5 Impact of sweep Λ_1 on trim drag

Along with the increase of Λ_1, the $\Delta C_{D\_tr\_p}$ decreases since the outer wing area and moment arm of the control surface C increase, thus reducing the δ_C for trim. The $\Delta C_{D\_tr\_w}$ is negative and it increases with the increase of Λ_1, which means the spanwise lift distribution is improved. But the beneficial effect decreases with the increase of Λ_1. The minimum and maximum of C_{D_trim} occur at $\Lambda_1=40°$ and $\Lambda_1=47.5°$, respectively. When Λ_1 is larger than 47.5°, the trim drag decreases gradually.

2.3.2 Impact of outer wing leading edge sweep

The impact of Λ_2 on C_{D_trim} is shown in Fig. 6. When the pitching moment arm of control surface C increases, the C_m decreases. Therefore, the $\Delta C_{D\_tr\_p}$ decreases with the increase of Λ_2 until Λ_2 is more than 32.5°, and then it increases gradually. Consequently, the δ_C for trim decreases and approaches zero when $\Lambda_2=32.5°$. The $\Delta C_{D\_tr\_w}$ is negative when Λ_2 is less than 32.5°, while it turns to positive when Λ_2 is more than 32.5°. This indicates that the spanwise lift distribution is improved, but the beneficial effect diminishes with

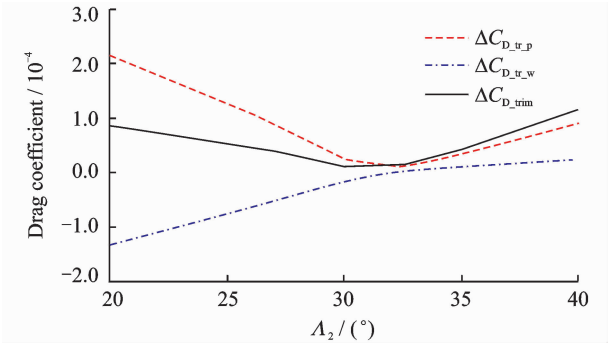

Fig. 6 Impact of sweep Λ_2 on trim drag

the increase of Λ_2. The C_{D_trim} decreases until Λ_2 is larger than 32.5°.

2.3.3 Impact of aspect ratio

The impact of aspect ratio AR on C_{D_trim} is illustrated in Fig. 7. The $\Delta C_{D\_tr\_p}$ decreases until AR exceeds 5.25. After that it increases gradually. It is due to the fact that the span and pitching moment arm of control surfaces C increase. Moreover, the C_m decreases from positive to negative. Consequently, the δ_C for trim decreases and approaches zero at $AR=5.25$. The $\Delta C_{D\_tr\_w}$ increases gradually when the AR increases. It changes from negative to positive when AR is larger than 5.25. The whole effect is that the C_{D_trim} decreases until AR is more than 5.25, and it reaches the minimum at $AR=5.25$.

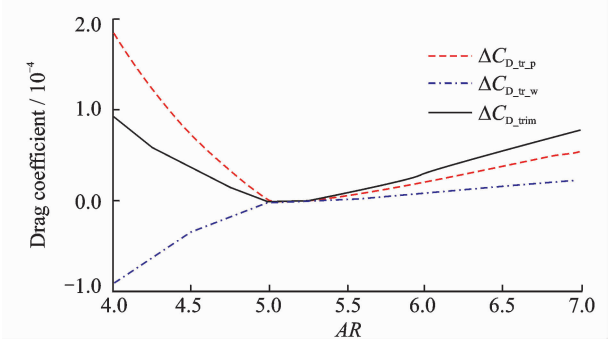

Fig. 7 Impact of aspect ratio on trim drag

3 Conclusions

The quantitative investigations of the trim drag for the BWB UAV have the following conclusions:

(1) Regarding to the allocations of control surfaces for trim, although the option "Hybrid" has the minium trim drag, the option C can simplify the control system without remarkable trim-drag penalty.

(2) The position of gravity center has a primary impact on the trim drag, which rapidly decreases with the backward movement of gravity center. When $\bar{x}_{cg}$ is 0.2, the trim drag is minimal.

(3) The planform parameters have secondary impacts on the trim drag. Careful selections of the planform parameters can further reduce the trim drag by 1 to 4 counts.

Acknowledgements

This work was supported by the National Defense Basic Scientific Research Program of China (No. A2520110006) and the Fundamental Research Funds for the Central Universities (Nos. NJ20130001, NJ2012014).

References:

[1] Liebeck R H. Design of the blended wing body subsonic transport[J]. Journal of Aircraft, 2004, 41(1): 10-25.

[2] Qin N, Vavalle A, Le Moigne A. Spanwise lift distribution for blended wing body aircraft[J]. Journal of Aircraft, 2005,42(2):356-365.

[3] Lyu Z, Martins J R. Aerodynamic shape optimization of a blended-wing-body aircraft [R]. AIAA 2013-0283, 2013.

[4] Lee D S, Gonzalez L F, Auld D J, et al. Aerodynamic/RCS shape optimisation of unmanned aerial vehicles using hierarchical asynchronous parallel evolutionary algorithms[R]. AIAA 2006-3331, 2006.

[5] Kuntawala N, Hicken J, Zingg D. Preliminary aerodynamic shape optimization of a blended-wing-body aircraft configuration[R] AIAA-2011-642, 2011.

[6] Roskam J. Airplane design, Part 6 [M]. Ottawa, Kansas: Roskam Aviation and Engineering Corporation, 1985:311-312.

[7] You Lianxing, Yu Xiongqing, Ouyang xing. Parametric geometry modeling for conceptual design of high supersonic unmanned aerial vehicles[J]. Journal of Nanjing University of Aeronautics & Astronautics, 2014, 46(3): 425-432. (in Chinese)

[8] Zhang Zhenming, Liu Yi, Ding Yunliang. Parametric geometry modeling and shape optimization method for hypersonic flight vehicles[J]. Journal of Nanjing University of Aeronautics & Astrnautics, 2012, 44(2): 172-177. (in Chinese)

[9] Carmichael R L, Erickson L L. PAN AIR—A higher order panel method for predicting subsonic or supersonic linear potential flows about arbitrary configurations[R]. AIAA-1981-1255, 1981.

[10] Jin R, Chen W, Simpson T W. Comparative studies of metamodeling techniques under multiple modeling criteria [J]. Journal of Structural and Multidisciplinary Optimization, 2001, 23(1):1-13.

(Executive editor: Zhang Tong)